Analysis of the Dynamical Behavior of Coherent Structures in In-Cylinder Flows of Internal Combustion Engines

Jorge Raposo, Werner Hentschel
Research & Development,Volkswagen AG, Germany

Wolfgang Merzkirch
Lehrstuhl für Strömungslehre, GH University of Essen, Germany

ABSTRACT

In this article the use of two coherent structure identification methods to analyze the in-cylinder flow is described. The techniques - Proper Orthogonal Decomposition (POD) and the Discrete Wavelet Transform (DWT) – were chosen to be used as velocity averaging techniques to investigate the problem of cyclic variations on in-cylinder flows. The POD and DWT averaging methods are described and used with experimental velocity data. As a test case, two dimensional velocity measurements performed with Particle Image Velocimetry (PIV) on a water analog test bed were used.

The results obtained offer a new way of analyzing in-cylinder flows. The POD decomposition technique provides a classification method based on an energy criterion by which the mean flow is seen as a superposition of coherent structures. From their temporal coefficients it is possible to characterize its dynamical behavior. The DWT is useful in delivering local information without performing too much smoothing. It can be used to identify instability areas in the flow at several scales.

1. INTRODUCTION

As showed by many researchers large-scale vortical structures play an important role in the dynamics of turbulent flows. This is particularly true for the flow inside the combustion chamber of an internal combustion (IC) engine. As the mixing process inside an IC engine is strongly dependent on global flow structures, such as swirl and tumble, inducted during the intake stroke, the understanding of the dynamics of these structures is fundamental to improve the combustion process and consequently, reducing the emissions and consumption levels.

The stratified charge spark ignition (SI) engine is a new combustion concept with the potential to increase engine performance and meet the increasingly stringent environmental legislation, Spicher *et al.* (1998). Contrarily to the homogenous charge SI engine, the gasoline is injected directly into the cylinder during the compression phase of the engine cycle.

Under part load operation, a lean combustion strategy is used to decrease fuel consumption. A small amount of gasoline is injected into the cylinder and under the action of the macroscopic in-cylinder flow an ignitable mixture is created and transported into the vicinity of the spark plug while the rest of the charge remains lean, Heywood (1988).

In order to realize this, the motion of the macroscopic flow structures must be stable enough to ensure a high repetitiveness throughout all cycles under a wide range of varying parameters like pressure, engine speed, load, etc. However, several experimental studies have shown, Young *et al.* (1981), Arcoumanis *et al.* (1987), Fansler *et al.* (1987), Reuss *et al.* (1999), Hentschel *et al.* (1998) and Mouqallid *et al.* (1998), that there are strong variations on the flow from cycle to cycle, even under motored conditions. As a consequence, the combustion process takes place under strong variations of the air-fuel ratio reducing drivability and increasing fuel consumption and pollutant gas emissions.

The exact causes for this phenomenon are not known. It is believed that instabilities in the flow during the intake phase create different bulk flow topologies. The pressure wave dynamics in the intake port, the recycled exhaust gases and the intake valve opening might be responsible for the flow instability. Towards the bottom dead center position of the piston (BDC), the generated large-scale flow seems to converge to a more or less defined structure. Both one-dimensional and two-dimensional velocity measurements confirm this behavior, Hentschel *et al.* (2000). Later, during the compression phase, the flow exhibits a smaller but still significant variation. The large-scale structures setup inside the cylinder, tumble or swirl, are both dominated by large vortical structures. Therefore, it is expected that the mean flow variations, are associated with the motion of their vortex cores.

Early work done by Arcoumanis *et. al.* (1987) and Gerber *et al.* (1985) showed that the variations

in the mean flow of a steady-state in-cylinder flow were caused by the Precessing Vortex Core (PVC). More recently, Volkert *et al.* (1998) and Keller *et al.* (1996) have studied the PVC of swirling flows comparing the two-dimensional flow field with the local velocity in a single point. They were able to relate the local variation in the mean flow on the point with the motion of the PVC.

The most recent experimental studies on engine flows using Particle Image Velocimetry have been focused on showing the cycle-to-cycle variations of the mean flow, Reuss *et al.* (1998), Reuss *et al.* (1999), Mouqallid *et al.* (1998*), Trigui et al.* (1998). The results showed that the ensemble mean flow was not representative for the instantaneous velocity maps. Only when cycle-by-cycle averaging (low-pass filtering) was used it was possible to obtain better approximations of the instantaneous velocity flow field.

However, as noted by some of the researchers, the choice of the cutoff frequency was done empirically. Furthermore, when applied to planar velocity data, the use of a single cutoff frequency (or spatially, a fixed wavenumber) cannot cope with the varying dimensions of large-scale vortices that occur for particularly unstable swirling flow configurations, *e.g*,, with small valve openings.

In order to decompose the flow into a mean and a fluctuating part, without an *a priori* definition of turbulence for in-cylinder flows, the ideal averaging procedure technique should analyze the velocity signal (in space and in time) at its various scales and, using a physically based criterion, separate both components of the velocity.

Based on the concept of coherent structures, several techniques have been developed to extract these structures from experimental and numerical data, Bonnet *et al.* (1998). Coherent structures can be identified by its significant energy content, by its association with a mean velocity gradient (not necessarily a vortex) and for maintaining its identity for several turnover times, Bonnet *et al.* (1996). They are associated with the large-eddy motion, what makes them important for turbulent transport and engineering applications. They can also be triggered, phase-locked and manipulated, what makes their modeling and control of technological value.

In this work, the POD technique and the DWT were selected. The POD technique provides a linear approximation of a function enabling an easier characterization of the flow as a sum of weighted flow fields. The DWT on the other side was chosen because of its ability to adapt the smoothness degree depending on the local properties of the velocity. This could be a necessary premise to future analysis on transparent engines.

As a first step, these methods will be used on a steady state water analog test rig. This test section provides an excellent test case for future engine flows. For comparison purposes, the topology of the flow is similar to the one found at BDC on a real engine, Trigui *et al.* (1996) and Faure *et al.* (1998). It is important to note that this is the only possibility of obtaining two-dimensional velocity data with sufficient temporal resolution and optimal accuracy.

In addition, with a view to an application under real conditions on an engine, the measured data can be adapted to simulate the measured data from a transparent engine and test previously its robustness.

2. EXPERIMENTAL SETUP

The water analog test rig is an optically accessible device used to simulate the in-cylinder flow field during the intake process. The working fluid is water instead of air. Such a system offers an accurate simulation of the intake flows, provided that the Reynolds number is matched with that of the air.

A schematic representation of the test section is depicted in Figure1.

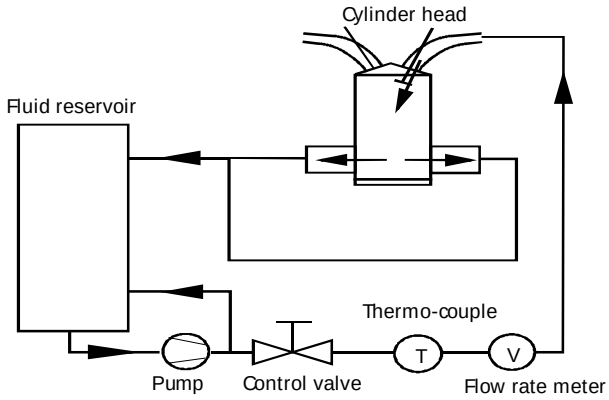

Figure 1. Water analog test section.

For a constant flow rate the two-dimensional flow field in a plane perpendicular to the cylinder axis located 30 mm under the cylinder head was measured. To enable the study of various flow topologies, the valve opening was varied from 1 mm to 10 mm.

The measurements were performed with a PIV system described in Freek *et al.* (1998). This system allowed a 25 Hz sampling of the flow and thus guaranties a good temporal tracking at low flow velocities. During the measured time (4 sec) 100 vector maps were obtained, each consisting of about 400 velocity vectors.

3. VELOCITY DECOMPOSITION

3.1. Proper Orthogonal Decomposition

The Proper Orthogonal Decomposition (POD) or Karhunen-Loeve expansion provides the best linear approximation of a function with the smallest mean

square error, Berkooz *et al.* (1993). Because its base functions are obtained through the minimization of a functional involving the solution of an eigenvalue problem, the resulting decomposition is not biased by *a priori* defined base functions. This is important because it has been argued that the use of Fourier base functions, due to its regularity, is not optimal to decompose turbulent signals. Another advantage of using POD to decompose the velocity is that is allows a decoupling of the time and space variables within each term of the decomposition. This is an essential feature to understand the dynamical behavior of the large-scale structures.

Let u(x,y,t) be a two dimensional velocity field with M grid points at a time instant t, t=1,...,N. Following the snapshot POD construction described by Fiedler *et al.* (1999) we can build a time dependent vector $\vec{a}_i$ based on the whole N snapshots,

$\vec{a}_i = (u_{i,1}, u_{i,2}, ..., u_{i,N})$.

The 2D snapshot POD looks for the coordinate system $\vec{y}$ which optimally represents $\{\vec{a}_i\}$, i=1,..,M. This corresponds to maximizing the following sum:

$$l_k = \sum_{i=1}^{M} (\vec{a}_i \cdot \vec{y}_k)$$

with k=1,..,N possible values. This leads to an eigenvalue problem where λ_k are the eigenvalues. Sorting the eigenvalues in a decreasing order and computing their respective eigenvectors we obtain N linearly independent vector fields or modes y_k. It can be shown that the eigenvalues represent parcels of the flow field energy, Berkooz *et al.* (1993). By definition of a coherent structure:"...which contains the most energetic part of the flow" it is simple to select the first q modes that contain, *e.g.*, 90% of the flow energy. In this way we obtain:

$$u(x,y,t) = \bar{u}(x,y,t) + u'(x,y,t) =$$
$$\underbrace{A_1(t)y_1(x,y) + A_2(t)y_2(x,y) + ... + A_q(t)y_q(x,y)}_{\bar{u}(x,y,t)} +$$
$$+ \underbrace{... + A_{q+1}(t)y_{q+1}(x,y) + A_N(t)y_N(x,y)}_{u'(x,y,t)}$$

Eq. 1

From the experimental data it was found that with q=2 it is possible to represent more than 92% of the flow energy. From Eq. 1 it follows:

$$\bar{u}(x,y,t) = A_1(t)y_1(x,y) + A_2(t)y_2(x,y)$$

Eq.2

3.2. DISCRETE WAVELET TRANSFORM

Another way of approximating turbulent velocity signals is to decompose it using Wavelet analysis. Although it uses predefined base functions (wavelets), their regularity can be adjusted to resemble as most as possible to the original turbulent signals. In addition, it provides *per si* a scale decomposition rendering an automatic appreciation of the energy distribution along the various turbulent scales (time and space) Farge *et al.* (1992). This gives an extra degree of freedom when decomposing a velocity field. It also allows the analysis of non-stationary flows because it performs the energy decomposition locally and does not integrate it along the full time to which the velocity signal belongs.

This technique has been chosen with the aim of applying it to decompose the velocity fields obtained from measurements on transparent engines where the non-stationarity of the flow from cycle-to-cycle is evident. For these cases the non-linear approximation given by the wavelet decomposition can better approximate the flow field as a linear decomposition technique like the POD.

At a time step t, u(x,y,t) is developed as an orthonormal wavelet series from the largest scale $l=2^0$ to the smallest scale $l=2^J$ using a two-dimensional multiresolution analysis:

$$u(x,y,t) = \sum_{j=0}^{J-1} \sum_{i_x=0}^{2^j-1} \sum_{i_y=0}^{2^j-1} \sum_{m=1}^{3} d^m_{j,i_x,i_y}(t) j^m_{j,i_x,i_y}(x,y)$$

Eq. 3

Here $j_{i,j}$ is the one-dimensional wavelet function. The coefficients are given by $d^m_{j,i_x,i_y}(t) = \left\langle u(x,y,t), j^m_{j,i_x,i_y}(x,y) \right\rangle$ where $\langle , \rangle$ denotes the inner product. Note that u(x,y,t) is also a sum of linearly independent parcels but in this case the coefficients are not ordered by its energetic value. They span all the scales (position and frequency) in the flow for a specific time instant t. The analysis has to be repeated for all the N time instants. This means that first a 2D wavelet decomposition is performed independently of the time step. Later, the coefficients $d^m_{j,i_x,i_y}(t)$ are also wavelet decomposed but this time in time and one-dimensionally.

Contrary to the POD, the wavelet analysis does not sort by itself the decomposition by its energetic values. Therefore, an energy criterion must be devised for the wavelet decomposition. This implies the screening and elimination of all coefficients that are smaller than a pre-defined threshold. The value of this threshold is determined by analyzing the energy distribution curve of the signal. This process leads to the following decomposition:

$$\bar{u}(x,y,t) = \sum_{j=0}^{J-1} \sum_{i_x=0}^{2^j-1} \sum_{i_y=0}^{2^j-1} \sum_{m=1}^{3} d^{m}_{j,i_x,i_y}(t)\, j^{m}_{j,i_x,i_y}(x,y)$$

Eq. 4

with $d^{m}_{j,i_x,i_y}(t) > e$, where all $d^{m}_{j,i_x,i_y}(t) < e$ are set to zero. This is the essence of the non-linear approximation performed with wavelets. The coefficients are set to zero independently of its spatial location or scale.

4. RESULTS AND DISCUSSION

The results presented in Figure 2 show the mean flow as obtained through a POD decomposition given by Eq. 2. Figure 2 a) presents the first mode $y_1(x,y)$. It is the eigenvector field with the biggest projection over the total 100 vector maps. In the structure it is identical to the ensemble mean vector field. Figure 2 b) shows the second mode $y_2(x,y)$. It corresponds to the eigenvector field with the second biggest projection over the total 100 vector maps. The presence of an organized structure is clear. This structure superimposes on the mean flow to create a varying mean flow field.

When an ensemble average (or Reynolds decomposition) is calculated the variations in the mean flow caused by the structure of the second mode are given to the turbulent or fluctuating component of the velocity. By looking at the evolution of the temporal coefficients in Figure 2 c), it can be seen that an ensemble average of the temporal coefficient of the second mode $A_2(t)$ would yield an insignificant contribution of $y_2(x,y)$ to the flow field statistics. However, it is precisely the temporal evolution of the product $A_2(t)y_2(x,y)$ that, superimposed on $A_1(t)y_1(x,y)$, recreates the PVC motion observed in the measured flow field. This information has been so far obscured by the use of inappropriate velocity decomposition techniques.

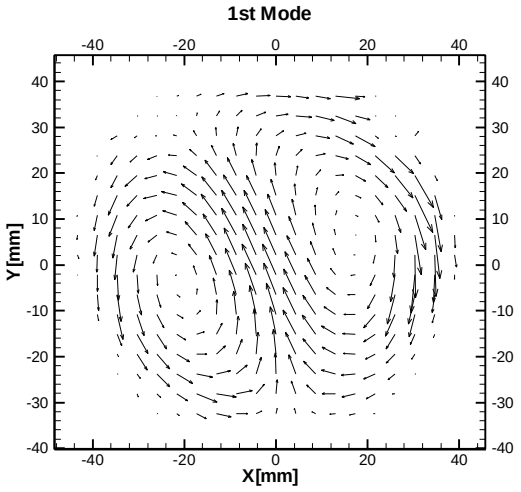

a)

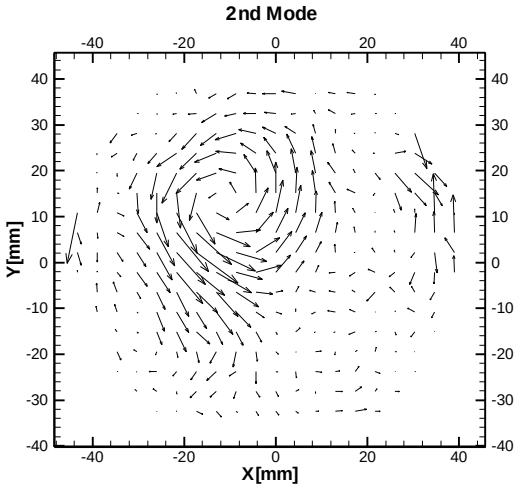

b)

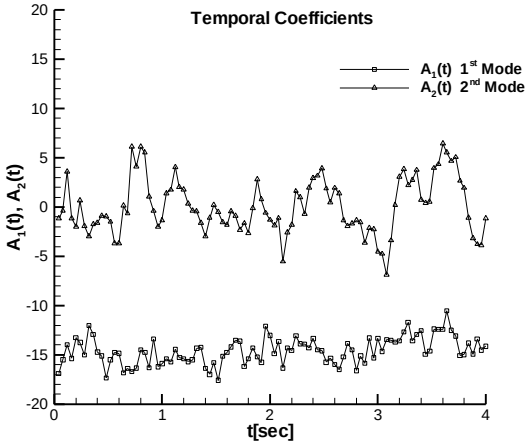

c)

Figure 2. **a**) First mode (eigenvector field) of a POD decomposition for a valve opening of 3 mm; **b)** Second mode (eigenvector field) of the POD decomposition for a valve opening of 3 mm. **c)** Temporal coefficients associated with the first two modes of the POD decomposition.

The velocity decomposition performed by the DWT is not appropriate to view the flow as a sum of weighted structures. Instead, its multi-scale signal decomposition allows a characterization of the mean flow based on its energy distribution through the spatial and temporal scales. As an example, in Figure 3 the spatial distribution of the smallest temporal scales present in the mean flow obtained through Eq. 3 is shown. These time scales represent the equivalent of a cutoff frequency in Fourier filtering. In areas of the flow where the mean velocity presents a higher variation the local energy distribution belonging to the mean flow spreads into higher frequencies. Not surprisingly, it shows that in the vicinity of the vortex center, where the local mean velocity presents a higher variation, the DWT

decomposition includes coefficients of small time scale.

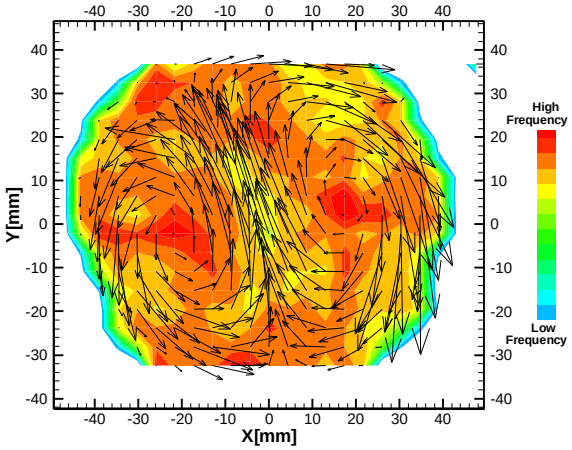

Figure 3. Distribution of threshold frequencies detected by the DWT over the measured plane for the total measured time. The dark areas signify areas of higher mean velocity variation.

A comparison between both decomposition techniques was done and, apart from particular time instants, the mean flow field obtained by each technique was practically identical. The differences encountered were associated with the appearance of a small third vortex into the mean flow. Because the existence of this vortex was restricted to only two vector maps of the whole 100 measured vector fields, a linear approximation technique like the POD does not represent well such singularities. To illustrate this, Figure 4 shows a comparison between the mean flow fields delivered by both techniques and the measured flow field at t=3.64 *sec*.

It can be seen in the instantaneous velocity field that the vortex on the right upper area of the graphic divides itself into two smaller vortices.

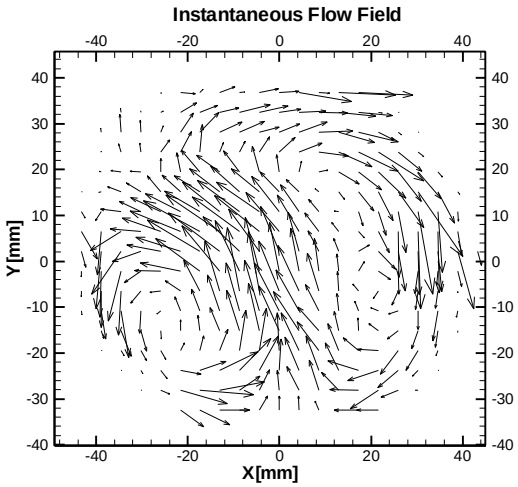

a)

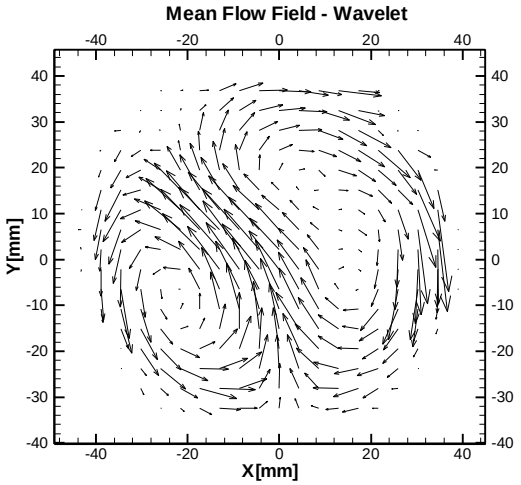

b)

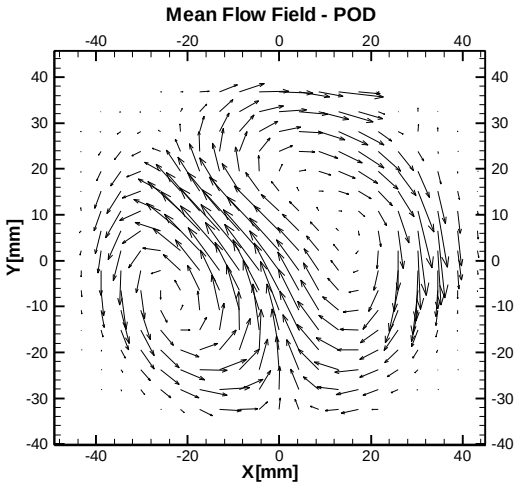

c)

Figure 4. a) Instantaneous velocity field measured at t=3.64 *sec*; **b)** Reconstructed DWT mean flow measured at t=3.64 *sec*; **c)** Reconstructed POD mean flow using the first two modes at t=3.64 *sec*.

The DWT reconstruction of the mean flow field provides a better approximation of the instantaneous flow field than the POD reconstruction. The former is able to reproduce the two vortices on the right upper area of the graphic whereas in the latter only a single deformed vortex appears. This example shows that although a linear approximation technique like POD provides allows a better understanding of the dynamical properties of the large-scale structures, in the presence of singularities in the flow topology the reconstructed flow field might be a too smoothed version of the real mean flow. For this reason, the non-linear approximation provided by the DWT should be used if the flow field under analysis shows a strong variation of its topology. It is expected that this should be the case for the in-cylinder flow of a real engine.

To illustrate the advantages of using the velocity decomposition techniques described in this work, different in-cylinder flow configurations were analyzed with respect to the dynamical behavior of the large-scale structures.

It is known from previous studies of steady state swirling flows on an engine cylinder that, as the valve opening increases, the flow topology evolves from a pair of counter rotating vortices with a highly irregular PVC motion to a stable single vortex structure.

In the following figures the dynamical behavior of the flow field obtained for three different valve openings is investigated. The results presented are obtained using the POD technique.

In Figure 5 a) and 5 b) the first two modes of the POD decomposition are shown for a valve opening of 1 mm.. The first mode shows the structure of the ensemble mean flow field and the second mode the structure which causes the deviation in the mean flow. By looking at Figure 5 c) the evolution of the temporal coefficient of the second mode quantifies the strong variation observed in the mean flow.

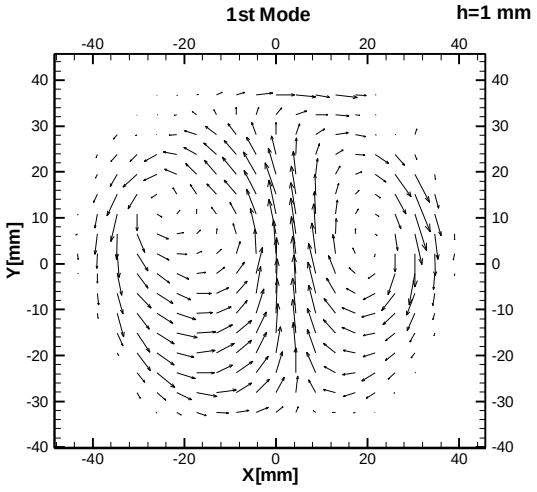

a)

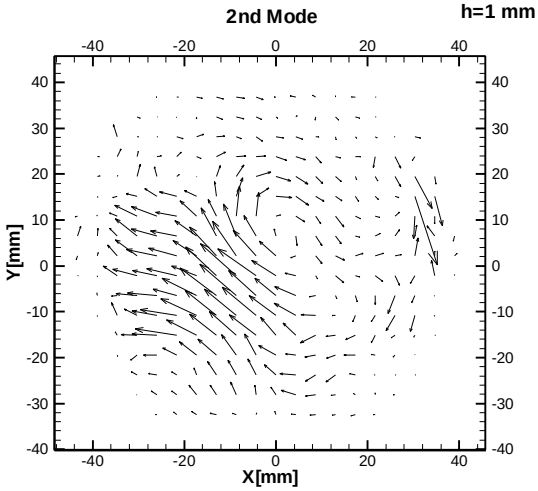

b)

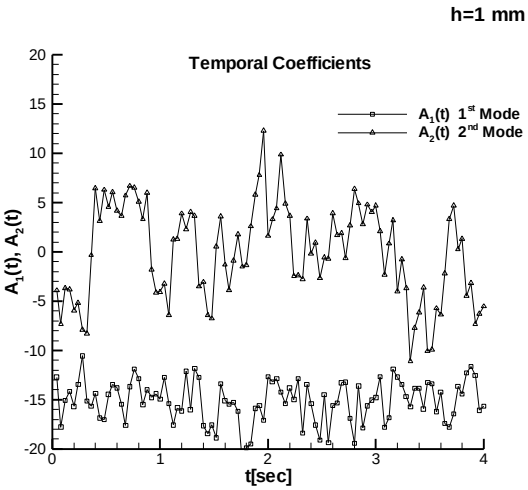

c)

Figure 5. **a)** First of the POD decomposition for a valve opening of 1 mm; **b)** Second mode of the POD decomposition for a valve opening of 1 mm; **c)** Temporal coefficients associated with the first two modes of the POD decomposition at a valve opening of 1 mm.

In Figure 6 a) and 6 b) the first two modes of the POD decomposition are shown for a valve opening of 5 mm. The first mode structure is still a pair of counter rotating vortices but the second mode has changes for each valve opening. Also the temporal coefficients indicate a more stable PVC motion of the mean flow.

Finally, in Figure 7 a) and b) the first two modes of the POD decomposition are shown for a valve opening of 9 mm. This valve opening produces the typical topology of a swirling flow. It corresponds to the most stable mean flow. Again the temporal coefficients can be used to quantify the degree of stability.

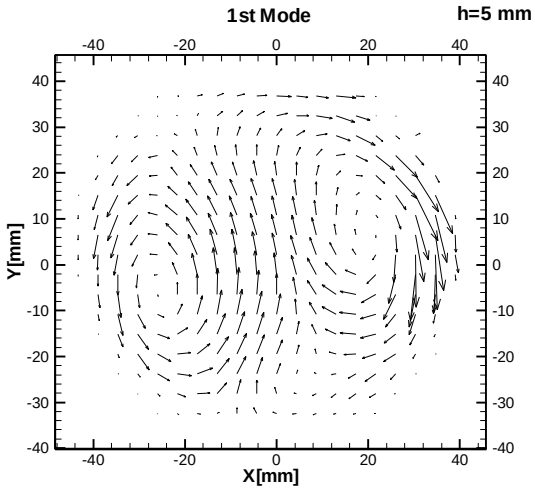

a)

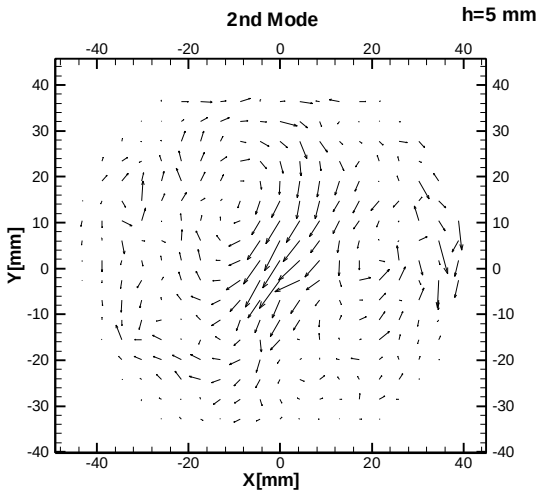

b)

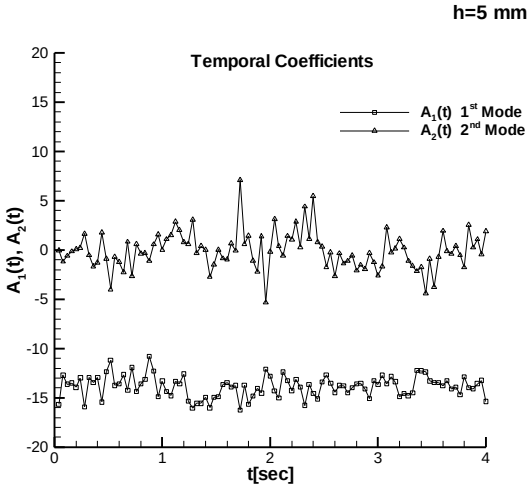

c)

Figure 6. **a)** First of the POD decomposition for a valve opening of 5 mm; **b)** Second mode of the POD decomposition for a valve opening of 5 mm; **c)** Temporal coefficients associated with the first two modes of the POD decomposition at a valve opening of 5 mm.

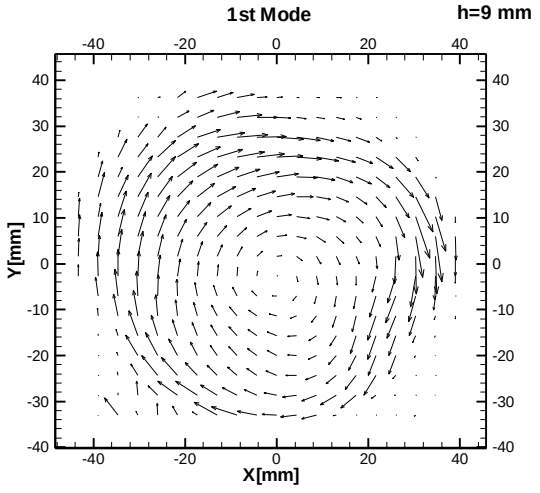

a)

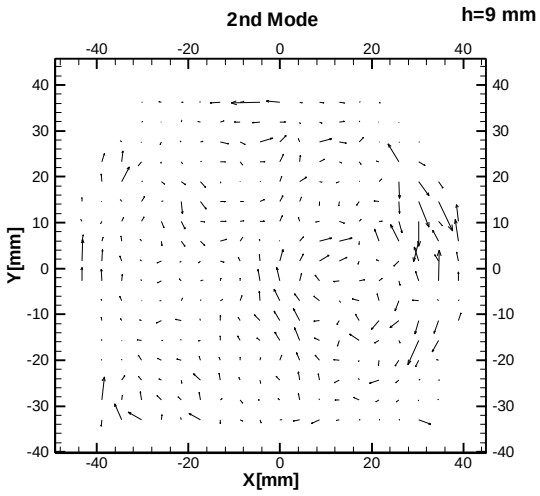

b)

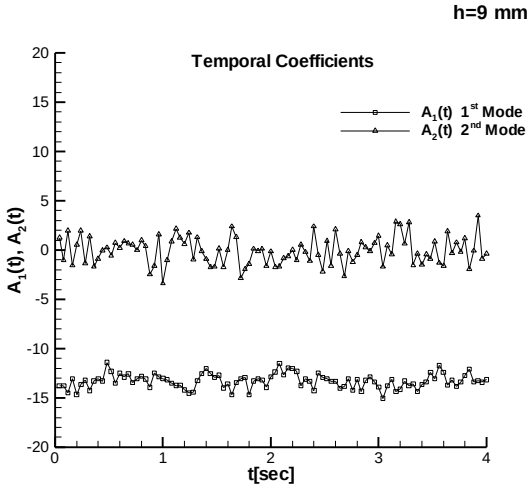

c)

Figure 7. **a)** First of the POD decomposition for a valve opening of 9 mm; **b)** Second mode of the POD decomposition for a valve opening of 9 mm; **c)** Temporal coefficients associated with the first two modes of the POD decomposition at a valve opening of 9 mm.

The information delivered by the POD decomposition allows a quantification and understanding of the variations in the mean flow that occur in the in-cylinder flow. The temporal coefficient of the second mode serves as an indicator of the dynamical properties of the mean flow. The typical frequencies for the motion of vortex cores can be taken from the curves of the temporal coefficients. It is also of notice that when the mean flow stabilizes the second mode structure responsible for the mean flow variation also vanishes.

5. SUMMARY AND CONCLUSIONS

In this work it was shown that alternative averaging techniques like the POD or the DWT provide a new way of information about the dynamical properties of the in-cylinder flow.

Making use of the coherent structure concept it is possible to determine a separation criterion with physical support. Furthermore, the identification and classification of a coherent structure can be used to analyse the cyclic variations present in the mean flow.

It is expected that the information obtained in this preliminary study can be applied to analize the cycle-to-cycle variations of the in-cylinder flow field in real engines.

ACKNOWLEDGEMENTS

The first author is a Marie Curie Fellow in the TMR programme financed by the European Commission and gratefully acknowledges this support.

REFERENCES

Arcoumanis, C., Haddjiapostolou, A., Whitelaw, J.H., 1987, Swirl Center Precession in Engine Flows, SAE Technical Paper Series 870370.

Berkooz, G., P. Holmes, J. L. Lumley., 1993, The proper orthogonal decomposition in the analysis of turbulent flows, Annual Review of Fluid Mechanics vol:25 pp.539-575.

Bonnet, J.P., a.o., 1998, Collaborative Testing of Eddy Structure Indetification Methods in Free Turbulent Shear Flows, Experiments in Fluids, vol:25 pp.197-225, Springer.

Bonnet, J.P., Lewalle, J., Glauser, M.N., 1996, Coherent Structures: Past, Present and Future, Proc. in Advances in Turbulence VI, pp.83-89 , Kluwer.

Fansler, T., French, D., 1987, Swirl, Squish and Turbulence in Stratified Charge Engines: LDA measurements and Implications for Combustion, SAE Technical Paper Series 870371.

Farge, M.., 1992, Wavelet Transforms and their Application to Turbulence, Annual Review of Fluid Mechanics vol:24 pp.395-457.

Faure, M. A., Sadler, M., Oversby, K. K., Stokes, J., Begg, S. M., Pommier, L. S., Heikal, M. R, Y.G., 1998, Application of LDA and PIV Techniques to the Validation of a CFD Model of a Direct Injection Gasoline Engine, SAE Technical Paper Series 982705.

Freek, C., Sousa, J.M.M., Hentschel, W., Merzkirch, W., 1999, On the Accuracy of a MJPEG-based Digital Image Compression PIV-System, Experiments in Fluids, vol:27 pp.310-320, Springer.

Gerber, A., Charnay, G., Bidault, M., 1985, Comparisons between Steady and Unsteady Flows in Cylinders of an Internal Combustion Engine, SAE Technical Paper Series 850121.

Hentschel, W., Block, B., Oppermann, W., 1999, PIV Investigation of the In-Cylinder Tumble Flow in an IC-Engine, Proc. of the EALA, pp. 429-438, Rome, Italy

Hentschel, W., Meyer. H., Stiebels, B., 2000: Einsatz laseroptischer Meßverfahren zur Unterstützung der Entwicklung von Brennverfahren mit Benzin-Direkteinspritzung. Proc. 4. Int. Symp. für Verbrennungsdiagnostik, Baden-Baden, pp. 181-196.

Keller, J., Volkert, J., Tropea, C., 1998, Influence of Axial Compression on a Strong Swirling Cylinder Flow, Proc. of the 9th Int. Symp. on App. of Laser Tech. To Fluid Mech., pp. 31.4.1-31.4.8, Lisbon, Portugal.

Mouqallid, M. Belghit, A., Trinite, M., 1998, Application of Cross Correlation Particle Image Velocimetry to the Charaterization of Unsteady Rotating Flow, Proc. of the 9th Int. Symp. on App. of Laser Tech. To Fluid Mech., pp. 31.2.1-31.2.9, Lisbon, Portugal.

Reuss, D.L., Rosalik, M., 1998, PIV Measurements During Combustion in a Reciprocating Internal Combustion Engine, Proc. of the 9th Int. Symp. on App. of Laser Tech. To Fluid Mech., pp. 37.1.1-31.1.17, Lisbon, Portugal.

Reuss, D.L., Rosalik, M., 1999, PIV Requirements for IC Engine Flows with Large Cyclic Variability, Proc. of the PIV'99 Symposium, pp. 217-224, Sta. Barbara, USA.

Spicher, U., Weimar, H.J., 1999, Die Benzin-Direktenspriztung: Zukunftstechnologie für den Ottomotor, Proc. Motorische Verbrennung-aktuelle probleme und moderne Lösungsansätze, Essen.

Trigui, N., Choi, W.-C., Guezennec, Y.G., 1996, Cycle Resolved Turbulence Intensity mesurement in IC Engines, SAE Technical Paper Series 962085.

Volkert, J., Tropea, C., Domann, R., Hübner, W., 1996, Combined Application of Particle Image Velocimetry (PIV) and Laser Doppler Anemometry, (LDA) to Swirling Flows under Compression, Proc. of the 8th Int. Symp. on App. of Laser Tech. To Fluid Mech., pp. 19.1.1-19.1.8, Lisbon, Portugal.